Enhancing the performance of soil microbial fuel cells by using a bentonite-Fe and Fe_3O_4 modified anode
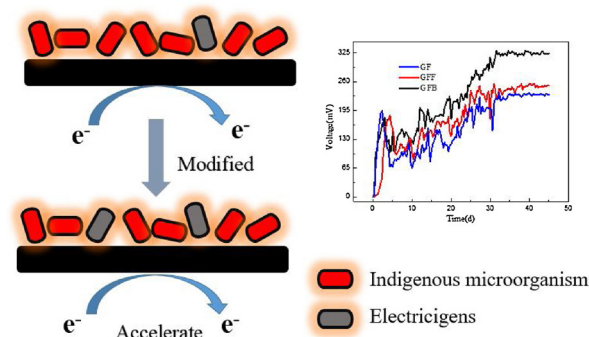
Bao Yu[a,b], Yanhong Li[a], Liu Feng[a,*]

[a] Department of Environmental Sciences and Engineering, Beijing University of Chemical Technology, Beijing 100029, PR China
[b] Center for Environmental Remediation, Institute of Geographic Sciences and Natural Resources Research, Beijing 100101, PR China

GRAPHICAL ABSTRACT

ARTICLE INFO

ABSTRACT

To improve the performance of soil microbial fuel cells (SMFCs), Fe_3O_4 and bentonite-Fe were selected as anode modifiers, and correspondingly, graphite felt (GF), GF + Fe_3O_4 (GFF), and GF + bentonite-Fe (GFB) anodes were created and applied to the SMFCs system. The stable voltages of SMFCs were 249 mV for GFF and 324 mV for GFB, thus representing an increase by 8.26% (GFF) and 40.87% (GFB) in comparison with those of GF. Moreover, the maximum power density in the modified treatment increased from 10.6 mW·m^{-2} to 18.28 mW·m^{-2} (GFF) and 29.98 mW·m^{-2} (GFB), and the internal resistance was reduced to 395 Ω for GFF and 219 Ω for GFB. The degradation efficiency clearly improved after being modified, especially by bentonite-Fe, and the removal ratios of the total petroleum hydrocarbon (TPH), anthracene, phenanthrene and pyrene reached 31.42%, 36.62%, 32.48% and 26.24%, respectively, after the SMFCs had run for 45 days. Both modifications contributed to the enrichment of electricigens on the anodes; however, there was minimal difference between them, which resulted in a similar microbial community on the modified anodes. The results demonstrated that Fe_3O_4 and bentonite-Fe could enhance the potential of SMFCs in soil remediation, and bentonite-Fe out-performed Fe_3O_4.

1. Introduction

Applications of soil microbial fuel cells (SMFCs) in organic contaminate soil remediation and energy conversion have attracted considerable attention [1,2]. SMFCs support the enrichment and metabolism of electricigens at the anode accompanied by the degradation

* Corresponding author.
    E-mail address: fengliu-buct@vip.sina.com (L. Feng).

of organic components and the generation of electrons, thus leading to an accelerated metabolic rate in anaerobic bacteria [3,4] and the occurrence of oxygen reduction reactions (ORR) at the cathode [5]. Currently, SMFCs are used mainly for two purposes: (1) to remediate organic contaminated soil [6], especially refractory organic pollutants, including petroleum hydrocarbons, phenol [7], and hexachlorobenzene (HCB) [8]; and (2) to provide power for low-power monitoring instruments or sensors [9,10]. Given that the emerging technology of SMFCs does not destroy soil structures and causes secondary pollution [11,12], SMFCs have wide potential applications in soil remediation [8,13].

Practical applications of SMFCs have been limited by their low power output. According to previous studies, many factors affect the performance of SMFCs, including electrode materials [14], electrode spacing [15], electrode layout [16], and reactor temperature [17]. Anodes play a remarkable role in the performance of the SMFCs and the characteristics of anode materials affect electricigens enrichment and electron transfer [18]. Schamphelaire et al. [19] confirmed that an anode is an important factor that affects the power generation of SMFCs. Song et al. [20] studied the effect of graphite felt and activated carbon fiber felt as SMFCs electrodes. Over the past decade, several carbon-based materials, including graphite felt, activated carbon felt, and carbon fiber cloth, have been used as anodes in SMFCs systems [7,20].

However, further research is required to promote the industrial applications of SMFCs, because the SMFC's voltage output was limited by the performance of traditional anode materials. Recently, modifications of anode materials have drawn significant attention from investigators [18]. Melamine has been used in anode modification to improve the microbial fuel cell (MFC) performance [21] and to increase the anode surface N/C ratio and positive charge; furthermore, negatively charged bacteria are easy to absorb. Lowy et al. [22] used metal ions and their oxides to modify graphite as an anode and found that the current density increased by 1.5- to 2.2-fold, thereby indicating that the reaction kinetic activity of the anode may increase given this modification. Previous studies have shown that modification plays an important role in promoting MFC performance. However, only a few studies on the anode modification in the SMFCs system have been conducted [18].

In the past decade, many different materials, including conductive polymers [23], carbon nanotubes [24], and metal ions and oxides [25,26], have been explored as anode modifiers. Metals and their oxides, such as Fe, Ni, and Mn, have been considered because of their easy preparation and cost-effective characteristics. In this report, iron materials have been selected as a modifiers; and these materials have also been applied previously to modify MFC electrodes [26,27]. To improve the performance of MFCs, Peng et al. [26] used a nano-Fe_3O_4 modified electrode (stainless steel active carbon); these authors found that the power generation performance of MFCs increased by 22%, thus suggesting that iron oxide (Fe^{3+}) plays an important role in the electron transfer process and enhances the activity of reaction kinetics. Fu et al. [28] modified the graphite anode with Fe/Fe_2O_3 to improve the anode kinetic activity and obtained a power density of 7.4×10^{-2} mW·cm^{-2}, which was 17.4 times higher than that of unmodified graphite. Their study showed that the presence of Fe effectively improved the anode reactivity of MFC [29].

Iron is a critical component of cytochrome C and iron-sulfur proteins, both of which are required by most electricigens and play a crucial role in the respiratory chain of microorganisms [30]. The iron oxides (Fe_3O_4/Fe_2O_3) are most commonly used as the modifier of anode, and zero valent iron (ZVI) is not used as a modifier. The iron oxides modification mainly improves the kinetics activity of the anode reaction. However, ZVI has excellent electrochemical activity. The electrode potential of ZVI is E_0 ($Fe^{2+}/Fe^0 = 0.44$ V). Thus, it can create a strong anaerobic environment that is beneficial to electron transfer. In addition, Fe(0) can provide electrons with promoted microbial growth

and metabolism as well as improve their activity [31]. The existence of Fe (0) will enhance the performance of SMFCs.

ZVI has been extensively used in the field of environmental remediation [32–34]. The disadvantages of ZVI lead to agglomeration and can cause environmental risks. ZVI has been loaded into other materials to maintain their original character and to enhance their stability [35,36]. Bentonite has been selected as a vector to support ZVI and has been shown to improve the dispersion and stability of ZVI particles and enhance the ability of composites due to the synergistic adsorption effect of bentonite [37–39]. To date, few studies has compared the differences in using iron with different valences as anode modifiers, and these have also rarely been applied to SMFCs.

In this work, Fe_3O_4 and bentonite-Fe were used to modify the anode for the first time, and the impacts of the modified SMFCs were thoroughly characterized. The SMFCs performance was evaluated in accordance with power generation efficiency and the degradation rate of organic contaminants. The effects of modification materials on SMFCs were comprehensively analyzed in accordance with anode electrochemical features, internal resistance and microbial community diversity. The choice of using a bentonite-Fe modified anode provided a novel concept for the future research direction for SMFCs and would promote further research of SMFCs electrode modification.

2. Materials and methods

2.1. Modified anode fabrication

GF and active carbon felt (Beijing Crystal Long Carbon Technology Co, Ltd, China) were used as the anode and cathode, respectively, and they were soaked in acetone for 24 h, washed with deionization water, and dried at 60 °C in a blast oven.

The Fe_3O_4 nanoparticles were prepared using the co-precipitation method according to Literature [26]. Bentonite-Fe nanoparticles were prepared using the method of KBH_4 reduction of Fe^{2+} using bentonite as a substrate [40,41].

Furthermore, 5 g Fe_3O_4 or bentonite-Fe was dissolved in 20 mL deionized water, and 2 mL polytetrafluoroethylene (PTFE) emulsion (60%, as a polymer binder) was added to the solution and then sonicated for 20 min to ensure the solution uniformity. Then, the materials of Fe_3O_4 and bentonite-Fe were evenly brushed on the GF. The anode materials of GF loading Fe_3O_4 (GFF) and loading bentonite-Fe (GFB) were dried at 60 °C and then was reserved for future used.

PTFE as a binder of materials, was used to enhanced the loading of Fe_3O_4, and bentonite-Fe and was loaded well on the GF, which was beneficial for the adhesion of microbial organisms [42].

2.2. SMFCs reactors and operation

In this experiment, three groups of SMFCs were constructed to research the performance of SMFCs and the effect of anode modification. Petroleum-contaminated soil was used to set up SMFCs. The properties of the soil was pH 7.56 and 6.23% organic matter content. The concentrations of TPH, anthracene, phenanthrene and pyrene were 11632, 219, 331 and 98 mg/kg, respectively.

A previous study [43] suggested that saturation moisture content increases the degradation of hydrocarbon, and the SMFCs are equipped with an air cathode system. The cathode was placed in the overlying water with the aim to promote H^+ transmission, and was maintained for a favorable soil anaerobic environment [2].

The air–cathode SMFCs consisted of a cylindrical type organic glass container with the dimensions D = 90 mm and H = 150 mm and were evenly loaded with 500 g contaminated soil (200 g + 300 g) with a thickness of 90 mm. Three groups of SMFCs were built in this experiment using GF, GFF and GFB as the corresponding anodes. In each reactor, the anode was buried in the soil; the cathode was horizontally installed at the water and soil interfaces. The anode and cathode were

Table 1
Experiment design of three groups SMFCs.

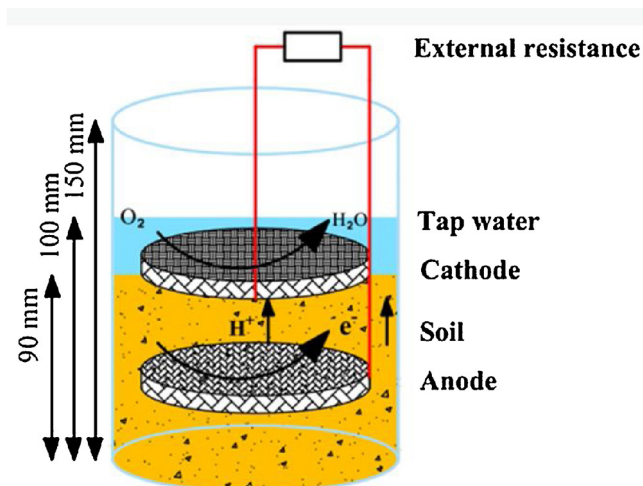| Groups	Anode	Cathode	Electrode area	Fe kg/m²	Code
1	Graphite felt	Active carbon felt	$5.67 \times 10^{-3}\,\mathrm{m}^2$	–	GF
2	Graphite felt + Fe₃O₄			3.744	GFF
3	Graphite felt + bentonite-Fe			0.707	GFB

Fig. 1. Experiment Schematic diagram of soil MFC.

connected through the wires, and the external resistance was 1000 Ω. During the running of SMFC, the depth of water in the cathode was 10 mm, and the water lost due to evaporation was compensated daily by topping it with tap water. The design of three groups of SMFCs is displayed in Table 1, and a schematic of the SMFCs is illustrated in Fig. 1. All of the SMFCs reactors were operated at a water bath temperature of 30 °C.

2.3. Material characterization

Cyclic voltammetry (CV) curves were obtained using an electrochemical workstation (chi660e) equipped with three electrodes. The test was conducted in a 50 mM phosphate solution with Ag/AgCl/KCl (3 M); Pt wire electrodes were used as auxiliary and counter electrodes and GF, GFF and GFB were used as working electrodes. The work electrode was scanned in the voltage range of −0.8 V~0.8 V, and the scanning speed was 20 mV s⁻¹. The anaerobic environment was established by N₂ bubbling, and the scanning time was 2 min each time. CV is a direct method for evaluating the electrical property of the electrode but its performance is not completely reflected in SMFCs.

The surface morphologies and internal structure of anode materials were examined by scanning electron microscopy (FEI Quanta250. USA). The acceleration voltage of the microscope was 15 KV, and the magnification was 2000×.

An X-ray diffraction (XRD) analysis was conducted on an X-ray diffractometer (Rigaku D/MAX 2500 VB2+/PC, Rigaku Company).

2.4. Determination and analysis

2.4.1. Voltage acquisition
The voltage changes in SMFCs were recorded every 2 min using an electrode data collector (Personal DAQ/56, IOTECH Co., Ltd., USA).

2.4.2. Polarization and power density curves
When the voltages had stabilized, the external resistance was adjusted from 100 Ω to 10,000 Ω, and each resistance was maintained for

30 min. We obtained the power density and polarization curves by recording the corresponding voltage value, and the maximum power density and internal resistance [44] were obtained through calculation and processing.

According to Ohm's law, the current (I, mA) is calculated by using I = U/R, where U (mV) is the cell voltage and R (Ω) is the external resistance. The formula for calculating the power density P (mW/m²) was presented as follows: P = U·I/(1000A·R), where A (m²) is the anode area.

2.4.3. Chemical analysis
The concentrations of TPH and three polycyclic aromatic hydrocarbons (PAHs): anthracene, phenanthrene and pyrene, in the soil samples were determined. The TPH of freeze-dried soil was through microwave extraction with an organic solvent [45]. The mixed solution of n-hexane and acetone (1:1) as the extracting agent and microwave digestion instrument (XH-800C) were used for digestion in the samples. The TPH concentration was determined through the constant weight method.

The extraction and determination of PAHs were performed as follows: 2.00 g freeze-dried soil (200 mesh) sample and 2 g anhydrous sodium sulfate were added to 25 mL of a hexane–acetone solution (volume ratio 1:1), which was then mixed evenly and microwaved. After microwave digestion was completed, the extraction solution was filtered through a 0.45 μm membrane, was purified using solid phase extraction cartridges (FL-PR), and then was volume-adjusted to 1 mL. A Shimadzu 2010 plus GC system was used to determine the PAHs concentrations. The GC with a flame ionization detector (FID) and its operating conditions were as follows: the capillary column DB-5 was 30 m × 0.25 mm × 0.25 μm; the injector temperature was 300 °C; and the FID temperature was 300 °C. The initial temperature of the capillary column was 100°C, where it remained for 2 min before it was raised linearly to 200 °C at a rate of 20 °C/min; then, it was further raised linearly to 280 °C at a rate of 10°C/min and was held for 5 min. High purity (above 99.99%) nitrogen was employed as a carrier gas. The sample was injected with no split, and the injection volume was 1 μL. The PAHs were identified from the retention times and characteristic ions of the identified compounds and were quantified through an external standard method at the peak area.

2.5. Microbial community diversity

At the end of the experiment, a biofilm sample around the anode electrode of each reactor was collected and dispersed into 10 mL of a sterile bottle. The microbial community diversity of the original and three anode soil samples were analyzed through high-throughput sequencing.

The universal bacterial primers 338 F (5′-ACTCCTACGGGAGGCAG CAG-3′) and 806R (5′-GGACTACHVGGGTWTCTAAT-3′) were used in a polymerase chain reaction (PCR) amplification. The PCR parameters were presented as follows: initial denaturation at 98 °C (3 min), followed by 27 cycles of 98 °C denaturation (30 s), 55°C annealing (30 s), and 72 °C extension (45 s), with a final extension at 72 °C (10 min), after which it was and then stored at 10 °C. The sequencing service was performed through an Illumina MiSeq platform at Personal Biotechnology Co., Ltd. (Shanghai, China). Clustering of sequencing into operational taxonomic units (OTUs) was performed using USEARCH software at 97% sequence identity.

3. Results and discussion

3.1. Anodic characterization

3.1.1. Composition analysis of the loading modifier
The XRD results of the GF, GFF and GFB materials are depicted in Fig. 2. GF was a reference that represents the graphite felt that was not
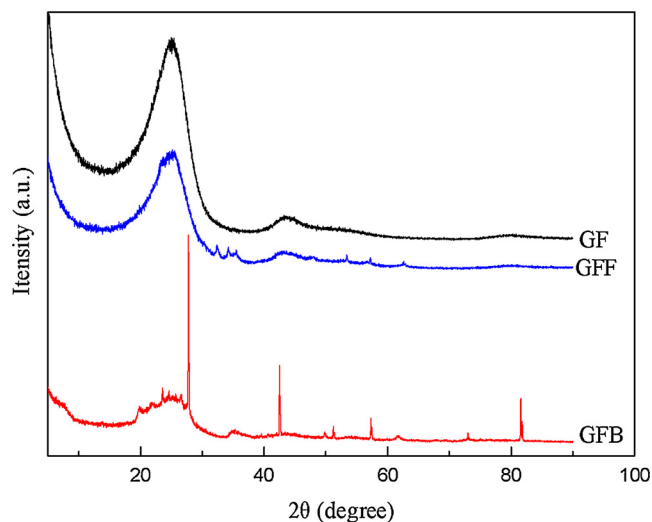
Fig. 2. X-ray diffraction (XRD) patterns of three anode materials: GF, GFF, GFB.

Fig. 4. Cyclic voltammetry curves of three anode materials: GF, GFF and GFB.

Fe than in Fe_3O_4.

modified and was used to analyze the load components on the two other electrodes. The XRD pattern of GFF exhibits the characteristic diffraction of Fe_3O_4 at 2θ of 35.5° (311: crystal plane index of the diffraction peak), 53.4° (422), 57.2° (511) and 62.6° (440). All such characteristic diffraction peaks can be indexed as Fe_3O_4, and the crystal structure was irregular with a minimal amount of impurities [46,47]. The 2θ that corresponds to the impurity peaks were 47.9°, 32.2°, and 34.2°, respectively. Those peaks areas were very small, and maybe they were the impurities associated with the production of Fe_3O_4.

GFB represents the GF modified by bentonite-Fe, and its composition was increasingly complicated. The corresponding 2θ values of the other diffraction peaks, except for the peak that corresponds to the main component bentonite, were 42.5°, 49.7°, and 73.04°, respectively, thereby indicating that Fe in the material was ZVI. According to the XRD analysis, GF was modified by bentonite-Fe and Fe_3O_4, and the component remained unchanged during the loading process.

3.1.2. Surface morphology of anodes

The SEM images of GF, GFF, and GFB are demonstrated in Fig. 3. The surface morphology of the anodized material before and after the bentonite -Fe and Fe_3O_4 modifications were observed using SEM. GF had a 3D macroporous structure and large specific surface area that consisted of graphite fiber with a diameter of approximately 20 µm with a smooth surface. Given the poor electrocatalytic properties of GF, the purpose of electrode modification was to improve its electrocatalytic properties and surface roughness. According to the figure, after modifying the GF, the graphite fiber surface roughness increased. The modifier was loaded evenly, and the load effect was better in bentonite-
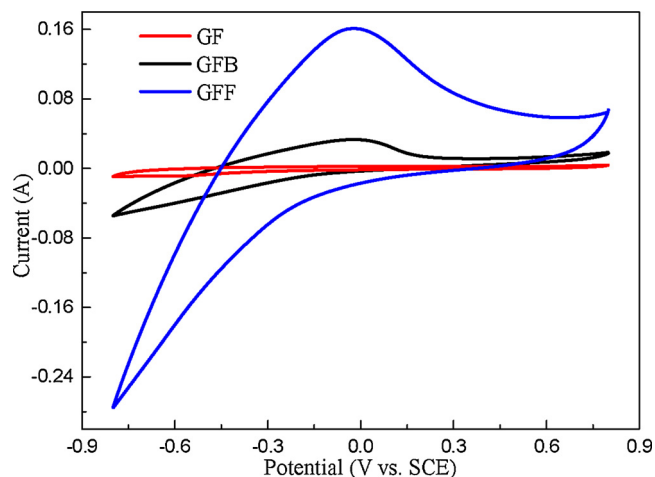
3.1.3. Electrochemical activity of anodes

The CV curves for GF, GFF, and GFB are exhibited in Fig. 4. According to the figure, a reduction peak at 639 mV for GF was found, and the corresponding current was 8.89 mA. The oxidation peaks of GFF and GFB were observed at 24 mV, and the corresponding peak currents were 161.1 mA and 33.3 mA.

An anode is the site of organic degradation (oxidation reaction). Thus, it plays an important role in the entire SMFCs system. The existence of a reduction peak did not increase the anodic half reaction activity, but the presence of the oxidation peak could catalyze the anodic reaction. The iron-modified materials showed an oxidation peak; therefore, the ability to catalyze the oxidation reaction was obviously improved because the two modifiers bentonite-Fe and Fe_3O_4 could have active anode reaction. These modifiers promoted the anode electron transfer and optimized the structure of the electrode surface; therefore, the currents were far greater in the GFF and GFB than in GF [48]. The results of CV scanning reflected the electrochemical properties of the anode electrodes, but the determined environment was located in the phosphate solution environment. The performance of GF, GFF, and GFB could be analyzed synthetically in accordance with the operation results of the SMFCs.

3.2. Effect of modifiers on the SMFCs performance

The running period of the SMFCs was 45 days. During the operation of the battery, three sets of SMFCs voltages varied with time, as displayed in Fig. 5(a). When the GFB, GFF, and GF began to run, the voltage increased rapidly and reached the local vertices within 4 days.
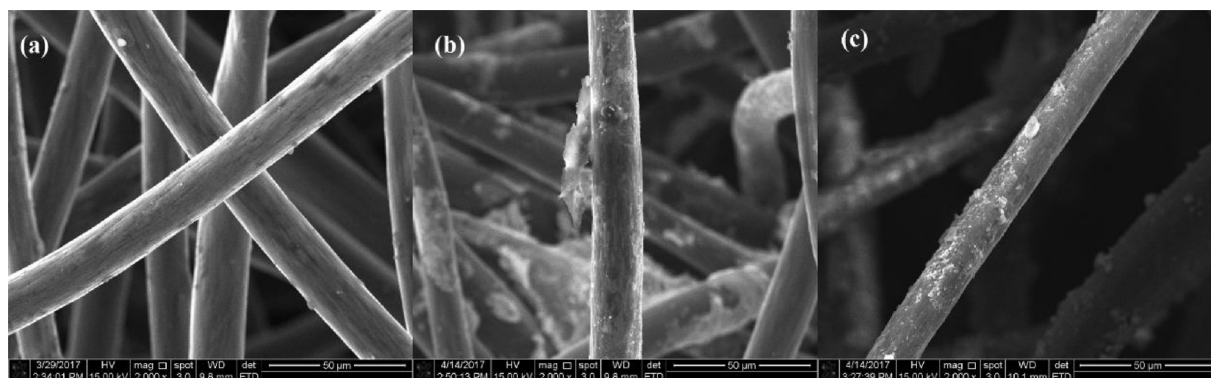

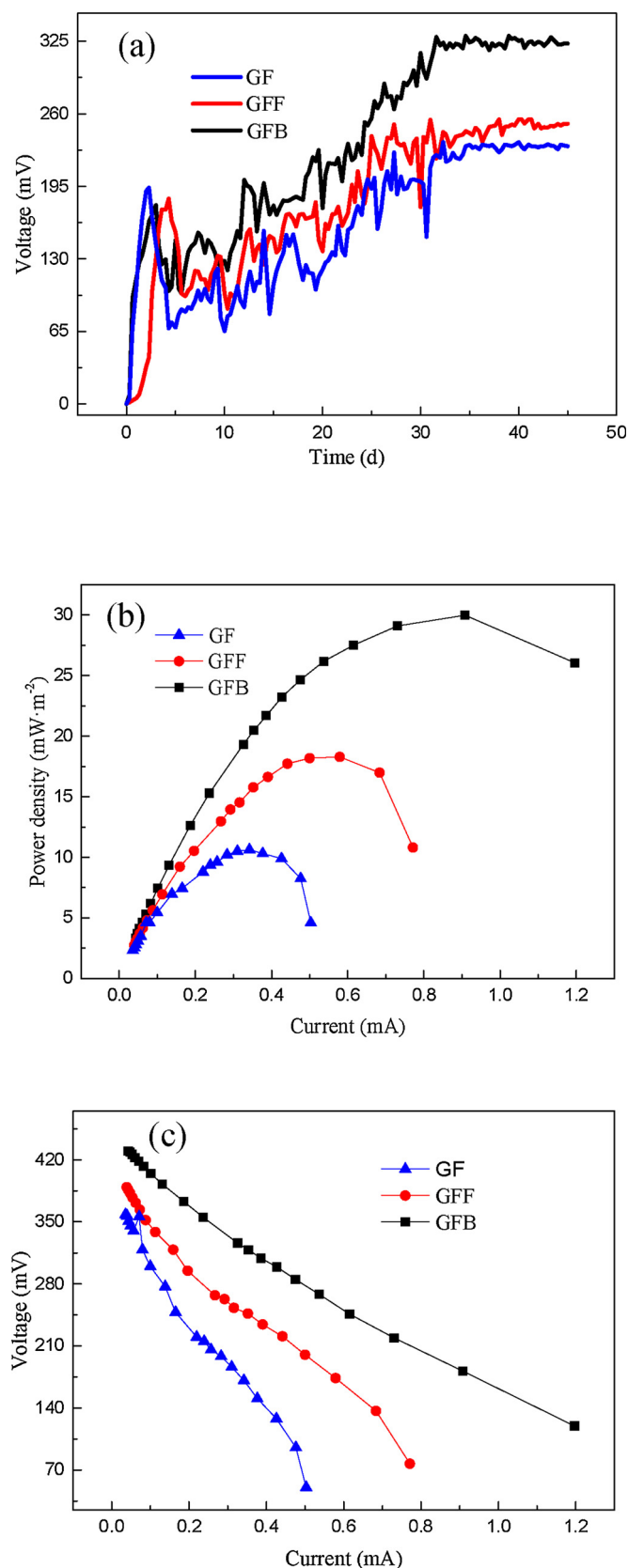**Fig. 3.** SEM images of three anode materials (a) GF, (b) GFF, (c) GFB.

Fig. 5. Electric performances of soil MFCs with different anode materials (a) voltage outputs, (b) power density curves, (c) polarization curves.

The vertices were 178, 184, and 193 mV for the GFB, GFF, and GF, respectively. The voltage then decreased for a period, but then slowly increased again. After 15 days, the voltages from the 3 groups were obviously different. The GFB had the highest voltage, and the overall trends showed that the voltage for each SMFC has constantly increased. The voltages of the 3 SMFCs reached their maximum and stabilized after approximately 32 days, with stable voltages of 324, 249, and 230 mV for GFB, GFF, and GF, respectively. The output voltage experienced a short period of rapid growth, declined, then gradually rose and finally reached stability. These changes in the SMFCs voltages were similar to the results of previous studies [49,50].

The early stage of the SMFC operations involved of enrich of the electricigens at the anode. Before setting up the SMFCs, a slow degradation reaction occurred in the soil. Given the lack of electron acceptors, the electrons generated by the degradation reaction accumulated in the soil; therefore, the voltages in the 3 groups increased sharply at the beginning, which was after building the SMFCs; this process is called electron release [6,7,15]. Then, the electrons in the soil continued to migrate to the anode. Simultaneously, the microorganisms continuously enriched around the anode and generated electrons through a decomposition of organic pollutants. Therefore, before completing the enrichment of microorganisms, the voltage of SMFCs generally showed an upward trend and a local fluctuation [51]. The electricigens were enriched on an anode while the SMFCs were running, and the voltages of the three SMFCs showed a difference. The performances were better in GFF and GFB than in the untreated GF, and the power generation was better in the GFB than in the GFF anode. In the late stage of operation, after completing the enrichment of the electricigens and ensuring their steady growth at the anode, the voltages of the three groups stabilized. The maximum cell voltages of GFB, GFF, and GF were stabilized at 324 mV, 249 mV, and 230 mV, respectively. The total charge outputs of the three group's SMFC were 900 C (GFB), 704 C (GFF), and 631 C (GF).

According to the voltage of the SMFCs, the stabilized voltage of GFB and GFF increased by 40.87% and 8.26%, correspondingly, relative to the 230 mV generated by the unmodified MFC. The results show that the Fe_3O_4 and bentonite-Fe modified anodes improved the electrical properties of SMFCs and that the performance of the bentonite-Fe modified anode was improved. According to the CV and voltage carves, the bentonite-Fe modified anode is suitable for the SMFCs system. Park et al. [52] used Mn^{4+} and Fe^{3+} modified anodes to significantly increase the voltage output, and the experimental results showed that the current increased by 1000 times when the intermediate electronic mediator was fixed on the graphite anode. Bentonite -Fe and Fe_3O_4 might also act as intermediate electron mediators and then accelerate the transfer of electrons. Bentonite-Fe might be superior to Fe_3O_4 given the property of ZVI. The strong reducibility of ZVI provided an anaerobic environment for the anode; thus, the electrons were not consumed at the anode; ZVI could donate electrons, which benefitted the initiation of the SMFCs, thus creating a strong electrochemical activity.

When the voltage had reached the steady state, the power density and polarization curves of the three SMFCs were obtained by adjusting the external resistance, as presented in Fig. 5(b) and (c). The maximum power densities for SMFCs with GFB, GFF and GF are 29.98, 18.28, and $10.60 \, mW \cdot m^{-2}$, respectively. In comparison with the GF group, the maximum power density of GFB and GFF increased by 182.83% and 72.45%, respectively. The performance of different cells can be evaluated by comparing their maximum power density. Sherafatmand et al. [6] used SMFCs to remediate PAHs-contaminated soil, and the maximum power density obtained under aerobic conditions was $8.67 \, mW \cdot m^{-2}$. An et al. [53] researched the performance of sediment microbial fuel cells according to the depth of the embedded anode, and the maximum power density was $14.5 \, mW \cdot m^{-2}$. Li et al. [4] utilized carbon fiber to improve the performance of the fuel cell deposits with the maximum power density of $17.3 \, mW \cdot m^{-2}$. Compared with the above research [4,6] and our previous study ($12.1 \, mW \cdot m^{-2}$) [15], the

Table 2
Electric performance summary of three SMFCs with different anode.

Code	Time/d	voltage/mV	Charge/C	P_{max}[a]/mW·m^2	Internal resistance/Ω
GFB	45	324	900	29.98	291
GFF	45	249	704	18.28	395
GF	45	230	631	10.6	610

[a] P_{max}, maxi SMFCs reactors and operation mum power density.

performance of SMFC after anode modification was been greatly improved. These results showed that bentonite-Fe and Fe$_3$O$_4$ play important roles in SMFCs, modifying the anode can effectively increase the maximum power density of SMFCs. Huang et al. [7] and Cao et al. [8]researched organic pollutants biodegradation and bioelectricity generation using a soil microbial fuel cell, and the maximum power density was 29.45 mW·m^{-2} and 77.5 mW·m^{-2}, respectively. They provided the granular activated carbon layer or Pt catalyst for the anode, so those maximum power densities were higher, but those cost were also higher.

The SMFC performances are summarized in Table 2. The internal resistances of SMFC were obtained by the polarization curves (Fig. 5c). Linear fitting of the polarization curves data was achieved using the software of origin 8.5, and the internal resistances were obtained from the slope of fitted lines. The internal resistances were 292 Ω, 395 Ω, and 610 Ω for GFB, GFF, and GF, respectively. This result showed that Fe$_3$O$_4$ and bentonite-Fe modified anodes can effectively reduce the internal resistance, and the effect of bentonite-Fe was better than the effect of Fe$_3$O$_4$. The internal resistance was lower in GFB and GFF than was found in previous research results [7,16,54]. According to previous studies and the results of this work, anode modification could effectively improve kinetic activity, accelerate the transfer of electrons from the substrate and microorganism to the electrode, and decrease the charge transfer resistance of the electrode [21,22]. The changes in the anode surface properties was the main reason for reducing the diffusion resistance of the anode [26,28].

3.3. Removal of TPH and PAHs

This work evaluated the repair effect of SMFCs in accordance with the percentage of pollutant removal from the soil in the SMFCs. The removal ratios of TPH and the three major PAHs after the three groups of SMFCs were run 45 days are illustrated in Fig. 6. The removal ratios of TPH in SMFCs with GF, GFF and GFB were 26.53%, 28.03%, and 31.42%, respectively, thus indicating that SMFCs can effectively degrade TPH in the soil. The anode modified by bentonite-Fe and Fe$_3$O$_4$ significantly improved the TPH removal ratios in the short-term operation, and the anode modification effectively improved the SMFC degradation of organic pollutants, especially with the function of Fe material on the SMFCs. These results mean that a breakthrough for SMFC anode modification research. The removal ratios of anthracene, phenanthrene and pyrene in the GF group were 29.95%, 24.14%, and 21.62%, respectively. The removal ratios of anthracene, phenanthrene and pyrene were 31.56%, 28.53%, and 23.28% in the GFF group and were 36.62%, 32.48%, and 26.24% in the GFB group, respectively. According to the removal ratios of PAHs, the PAHs removal efficiency of SMFCs with anodes modified by the iron material was clearly improved. In addition, the degradation degrees were different given the structural differences among anthracene, phenanthrene and pyrene [6].

The TPH and PAHs degradation mechanisms in SMFCs were due to the anaerobic metabolic activity of the bacteria and electricigens bacteria that were enriched in the anode. The key factors that determine the degradation ratio of pollutants were the quantity and activity of the microorganisms, and the electron transfer rate at the anode. As mentioned above, the modified anode showed accelerated electron transfer and had a certain catalytic effect on the anode half reaction, both of
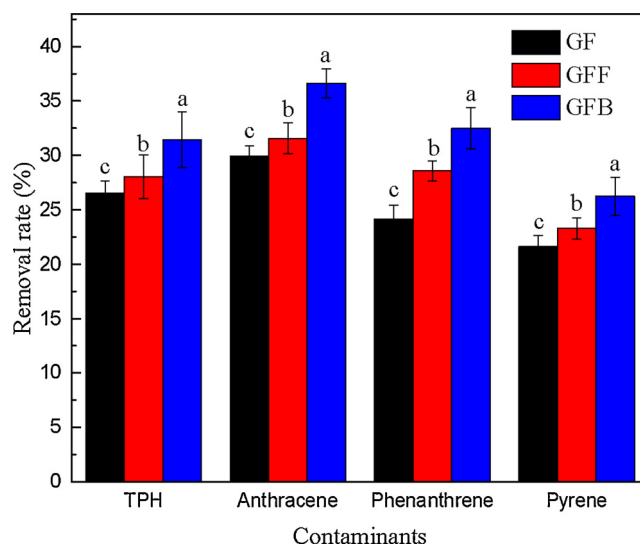

Fig. 6. Contaminants biodegradation performance in soil MFCs with different anode materials. Data was submitted to statistical analysis using Wilcoxon test at confidence limit of 95%. Different lower-case letters indicate significant difference (p < 0.05).

which improved the removal ratios of pollutants in the SMFCs. However, whether anodic modification could promote microbial enrichment on the anode and further improve the degradation of organic matter remained to be further determined by subsequent microbial community analysis.

3.4. Character of the microbial community

High-throughput sequencing of 16S rRNA gene was used to analyze the abundance and diversity of microbial communities, and information on the four samples is summarized in Table 3, including three anode soil samples in GFB, GFF, GF and the original soil (S).

The coverage of all four samples was higher than 0.994, thereby indicating that nearly all of the OTUs are covered and truly reflect the microbial community characteristics of the samples [55]. The sequences numbers were changed from 31,725 to 41,309 in the four samples. The OTUs number of original soil sample (716) was lower than those of anode samples (864–883). For four samples, the Shannon indexes ranged from 4.549 to 5.040, Simpson indexes ranged from 0.0163-0.0363; Chao1 values ranged from 890 to 994, and ACE values ranged from 855-986. In accordance with the Shannon and Simpson diversity indexes, the anode microbial community diversity is reduced and the uniformity is increased in the SMFC samples in comparison with the original soil samples [15]. In accordance with the Ace and Chao1 indexes, the abundance of microbes on the SMFCs anode was reduced [56].

Table 3
Species diversity and abundance indices of 4 samples.

Sample	Shannon[a]	Simpson[b]	ACE[c]	Chao1[c]	coverage	OTUs	Sequences
GFB	4.989	0.0167	986	994	0.995	871	36647
GFF	4.989	0.0165	973	971	0.996	883	41309
GF	5.040	0.0163	978	982	0.994	864	31725
S	4.549	0.0363	855	890	0.995	716	37850

[a] The species diversity index of microbial community. A higher number represents more diversity.
[b] The evenness index of microbial community. A higher number represents more evenness.
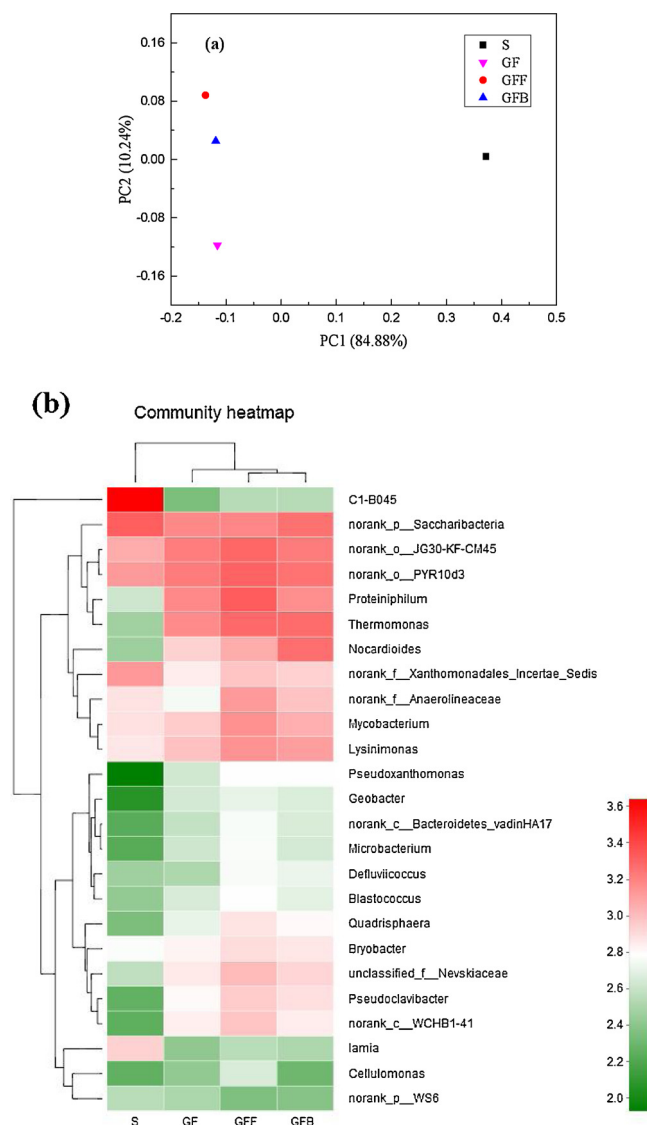[c] The abundance index of microbial community. A higher number represents more abundance.

Fig. 7. The results of microbial community diversity analysis (a) principal co-ordinates analysis, (b) heat map of the most abundant genera in the 4 samples, S: the original soil, GFF: soil from the GFF, GF: soil from the GF, GFB: soil from the GFB.

To analyze the main influential factors that affect the characteristics of microbial communities, the result of the principal coordinate analysis (PCoA) of the four samples at the OTUs level are depicted in Fig. 7(a).

The distance between the two points on the PCoA graph represents the degree of their similarity. In particular, a close distance indicates a similar composition of their microbial communities. According to the result, PC1 and PC2 contributed to 95.12% of the changes in microbial community characteristics. PC1 (84.88%, X-axis direction), the three groups of anode soil, showed obvious clustering and significant difference from the original soil, thereby indicating that the presence of SMFCs changed the microbial community structure, and was the main factor that affected the microbial community character.

The difference among the three groups of anodes (GFB, GFF, and GF) soil in the main component PC2 (10.24%, Y-axis direction) indicated that the anode material has a certain influence on the microbial community but had a weaker impact on community diversity than SMFCs existence. This finding is consistent with the analysis displayed in Table 3.

A heat map of the top 25 genera from the four soils is demonstrated in Fig. 7(b). The color depth indicates the relative abundance of the

genus. In comparison with the original soil, the characteristics of the anodic microbial communities of the three groups of SMFCs significantly differed but also had relatively small differences among the three groups of anode microorganisms. Considering the presence of SMFCs, the environment of soil had changed and the original dominant genera of the microorganisms were no longer competitive; here, the most obvious genera were *C1-B045* and *Lamia*. The relative abundance of C1-B045 was 13.12% in the original soil, which decreased to 0.99%, 0.87% and 0.73% in the anode of GFB, GFF, and GF, respectively. The relative abundance of lamia was 2.58% in the original soil, whereas the relative abundance in GFB, GFF and GF were 0.93%, 0.88%, and 0.86%, respectively.

The new dominant species were gradually highlighted. Among them, *Thermomonas*, *Proteiniphilum*, *Nocardioides*, *Pseudoxanthomonas* and *Geobacter* were the most prominent. The relative abundances in the original soil were 0.89%, 1.25%, 0.87%, 0.26% and 0.35%, and the corresponding microorganisms in the GFB, GFF, and GF groups were enriched by 3.28- to 6.4-fold. Those microbial should be related to the SMFCs power generation. In the previous research, *Proteiniphilum* and *Geobacter* has been found in SMFC or MFC systems as electricigens [15,57]. The relative abundances of *Thermomonas* were 5.4%, 4.85% and 4.93% in GFB, GFF and GF anode soil, and the relative abundances of *Nocardioides* were 5.27%, 2.89% and 2.84%, respectively. Notably, the relative abundance of *Nocardioides* and *Thermomonas* in the GFB group were higher than in other groups (GFF, GF), which indicated that bentonite-Fe modified anode is more conducive to the enrichment of microorganisms. Through the overall analysis of the heat map, the microorganism enriched effects were better in GFF and GFB than in GF.

4. Conclusion

After a graphite felt anode was modified by bentonite-Fe and Fe_3O_4, the power generation of SMFCs increased significantly, and the voltage increased by 40.87% and 8.3% in comparison with the SMFCs with the untreated anode. The maximum power density of GFB and GFF were 29.98 and 18.28 mW·m^{-2}, respectively. According to our experimental results, we found that bentonite-Fe and Fe_3O_4 effectively improved the performance of SMFCs and that bentonite -Fe was more effective than Fe_3O_4. The results of contaminant removal confirmed that modifications can improve the repair effect of SMFCs. Through electrochemical analysis (CV curves), polarization curves, and microbial community diversity analysis, bentonite-Fe and Fe_3O_4 can improve the SMFCs performance mainly by improving the electrochemical activity of the anode material, reducing the internal resistance, accelerating electron transfer, and promoting a microbial-enriched anode. However, the differences between bentonite-Fe and Fe_3O_4 on the microorganism enrichment were relatively minimal.

Acknowledgement

References

[1] X. Li, X. Wang, L. Wan, Y. Zhang, N. Li, D. Li, Q. Zhou, Enhanced biodegradation of aged petroleum hydrocarbons in soils by glucose addition in microbial fuel cells, J. Chem. Technol. Biotechnol. 91 (2015) 267–275.
[2] X. Li, X. Wang, Y. Zhang, L. Cheng, J. Liu, F. Li, B. Gao, Q. Zhou, Extended petroleum hydrocarbon bioremediation in saline soil using Pt-free multianodes microbial fuel cells, RSC Adv. 4 (2014) 59803–59808.
[3] H. Luo, G. Liu, R. Zhang, J. Song, Phenol degradation in microbial fuel cells, Chem. Eng. J. 147 (2009) 259–264.
[4] X. Li, X. Wang, Q. Zhao, L. Wan, Y. Li, Q. Zhou, Carbon fiber enhanced bioelectricity generation in soil microbial fuel cells, Biosens. Bioelectron. 85 (2016) 135–141.
[5] T.S. Song, Z.S. Yan, Z.W. Zhao, H.L. Jiang, Construction and operation of freshwater sediment microbial fuel cell for electricity generation, Bioprocess Biosyst. Eng. 34

(2011) 621–627.

[6] M. Sherafatmand, H.Y. Ng, Using sediment microbial fuel cells (SMFCs) for bioremediation of polycyclic aromatic hydrocarbons (PAHs), Bioresour. Technol. 195 (2015) 122–130.

[7] D.-Y. Huang, S.-G. Zhou, Q. Chen, B. Zhao, Y. Yuan, L. Zhuang, Enhanced anaerobic degradation of organic pollutants in a soil microbial fuel cell, Chem. Eng. J. 172 (2011) 647–653.

[8] X. Cao, H.L. Song, C.Y. Yu, X.N. Li, Simultaneous degradation of toxic refractory organic pesticide and bioelectricity generation using a soil microbial fuel cell, Bioresour. Technol. 189 (2015) 87–93.

[9] C. Donovan, A. Dewan, D. Heo, H. Beyenal, Batteryless, wireless sensor powered by a sediment microbial fuel cell, Environ. Sci. Technol. 42 (2008) 8591–8596.

[10] F. Zhang, L. Tian, Z. He, Powering a wireless temperature sensor using sediment microbial fuel cells with vertical arrangement of electrodes, J. Power Sources 196 (2011) 9568–9573.

[11] B.E. Logan, Exoelectrogenic bacteria that power microbial fuel cells, Nat. Rev. Microbiol. 7 (2009) 375–381.

[12] A. Zabihallahpoor, M. Rahimnejad, F. Talebnia, Sediment microbial fuel cells as a new source of renewable and sustainable energy: present status and future prospects, RSC Adv. 5 (2015) 94171–94183.

[13] T. Ewing, P.T. Ha, H. Beyenal, Evaluation of long-term performance of sediment microbial fuel cells and the role of natural resources, Appl. Energy 192 (2017) 490–497.

[14] K. Scott, I. Cotlarciuc, D. Hall, J.B. Lakeman, D. Browning, Power from marine sediment fuel cells: the influence of anode material, J. Appl. Electrochem. 38 (2008) 1313–1319.

[15] B. Yu, J. Tian, L. Feng, Remediation of PAH polluted soils using a soil microbial fuel cell: influence of electrode interval and role of microbial community, J. Hazard. Mater. 336 (2018) 110–118.

[16] Q. Zhao, M. Ji, R. Li, Z.J. Ren, Long-term performance of sediment microbial fuel cells with multiple anodes, Bioresour. Technol. (2017).

[17] H. Deng, Y.-C. Wu, F. Zhang, Z.-C. Huang, Z. Chen, H.-J. Xu, F. Zhao, Factors affecting the performance of single-chamber soil microbial fuel cells for power generation, Pedosphere 24 (2014) 330–338.

[18] J.M. Sonawane, A. Yadav, P.C. Ghosh, S.B. Adeloju, Recent advances in the development and utilization of modern anode materials for high performance microbial fuel cells, Biosens. Bioelectron. 90 (2017) 558–576.

[19] L. De Schamphelaire, K. Rabaey, P. Boeckx, N. Boon, W. Verstraete, Outlook for benefits of sediment microbial fuel cells with two bio-electrodes, Microb. Biotechnol. 1 (2008) 446–462.

[20] Ts. Song, Wm. Tan, Xy. Wu, C.C. Zhou, Effect of graphite felt and activated carbon fiber felt on performance of freshwater sediment microbial fuel cell, J. Chem. Technol. Bio. 87 (2012) 1436–1440.

[21] Ye. Xie, Z. Ma, H. Song, Z.A. Stoll, P. Xu, Melamine modified carbon felts anode with enhanced electrogenesis capacity toward microbial fuel cells, J. Energ. Chem. 26 (2017) 81–86.

[22] D.A. Lowy, L.M. Tender, J.G. Zeikus, D.H. Park, D.R. Lovley, Harvesting energy from the marine sediment-water interface II. Kinetic activity of anode materials, Biosens. Bioelectron. 21 (2006) 2058–2063.

[23] Yong Yuan, S. Kim, Polypyrrole-coated reticulated vitreous carbon as anode in microbial fuel cell for higher energy output, B. Korean Chem. Soc. 29 (2008) 168–172.

[24] Hao Ren, Soonjae Pyo, Jae-Ik Lee, Tae-Jin Park, Forrest S. Gittleson, Frederick C.C. Leung, Jongbaeg Kim, Andre D. Taylor, Hyung-Sool Lee, J. Chae, A high power density miniaturized microbial fuel cell having carbon nanotube anodes, J. Power Sources 273 (2015) 823–830.

[25] J.R. Kim, B. Min, B.E. Logan, Evaluation of procedures to acclimate a microbial fuel cell for electricity production, Appl. Microbiol. Biotechnol. 68 (2005) 23–30.

[26] X. Peng, H. Yu, X. Wang, Q. Zhou, S. Zhang, L. Geng, J. Sun, Z. Cai, Enhanced performance and capacitance behavior of anode by rolling Fe3O4 into activated carbon in microbial fuel cells, Bioresour. Technol. 121 (2012) 450–453.

[27] F. Zhou, Y. Litao, L. Kexun, G. Baochao, P. Liangtao, Z. Xi, The performance and mechanism of modified activated carbon air cathode by non-stoichiometric nano Fe3O4 in the microbial fuel cell, Biosens. Bioelectron. 74 (2015) 989–995.

[28] Y. Fu, Q. Xu, X. Zai, Y. Liu, Z. Lu, Low electrical potential anode modified with Fe/ferric oxide and its application in marine benthic microbial fuel cell with higher voltage and power output, Appl. Surf. Sci. 289 (2014) 472–477.

[29] D.R. Bond, D.R. Lovley, Electricity production by Geobacter sulfurreducens attached to electrodes, Appl. Environ. Microb. 69 (2003) 1548–1555.

[30] J. Li, H. Gao, A renewable potentiometric immunosensor based on Fe3O4 nanoparticles immobilized anti-igG, Electroanalysis 20 (2010) 881–887.

[31] B. Gu, D.B. Watson, L. Wu, D.H. Phillips, D.C. White, J. Zhou, Microbiological

characteristics in a zero-valent iron reactive barrier, Environ. Monit. Assess. 77 (2002) 293–309.

[32] N. Savage, M.S. Diallo, Nanomaterials and water purification: opportunities and challenges, J. Nanopart. Res. 7 (2005) 331–342.

[33] H. Ahn, H.Y. Jo, G.Y. Kim, K. Yong-Kwon, Effect of NaCl on Cr(VI) reduction by granular Zero Valent Iron (ZVI) in aqueous solutions, Mater. Trans. 53 (2012) 1324–1329.

[34] M.R. Olson, T.C. Sale, Charles D. Shackelford, C. Bozzini, J. Skeean, Chlorinated solvent source-zone remediation via ZVI-clay soil mixing: 1-year results, Ground. Water Monit. R. 32 (2012) 63–74.

[35] N. Efecan, T. Shahwan, A.E. Eroğlu, I. Lieberwirth, Characterization of the uptake of aqueous Ni2+ ions on nanoparticles of zero-valent iron (nZVI), Desalination 249 (2009) 1048–1054.

[36] R.A. Crane, T.B. Scott, Nanoscale zero-valent iron: future prospects for an emerging water treatment technology, J. Hazard. Mater. 211-212 (2012) 112–125.

[37] A.S.K. Kumar, R. Ramachandran, S. Kalidhasan, V. Rajesh, N. Rajesh, Potential application of dodecylamine modified sodium montmorillonite as an effective adsorbent for hexavalent chromium, Chem. Eng. J. 211-212 (2012) 396–405.

[38] Y. Li, Y. Zhang, J. Li, X. Zheng, Enhanced removal of pentachlorophenol by a novel composite: nanoscale zero valent iron immobilized on organobentonite, Environ. Pollut. 159 (2011) 3744–3749.

[39] Z.X. Chen, X.Y. Jin, Z. Chen, M. Megharaj, R. Naidu, Removal of methyl orange from aqueous solution using bentonite-supported nanoscale zero-valent iron, J. Colloid Interface Sci. 363 (2011) 601–607.

[40] Y. Li, Y. Zhang, J. Li, G. Sheng, X. Zheng, Enhanced reduction of chlorophenols by nanoscale zerovalent iron supported on organobentonite, Chemosphere 92 (2013) 368–374.

[41] Y. Zhang, Y. Li, X. Zheng, Removal of atrazine by nanoscale zero valent iron supported on organobentonite, Sci. Total Environ. 409 (2011) 625–630.

[42] T. Zhang, C. Cui, S. Chen, X. Ai, H. Yang, P. Shen, Z. Peng, A novel mediatorless microbial fuel cell based on direct biocatalysis of Escherichia coli, Chem. Commun. 21 (2006) 2257–2259.

[43] X. Wang, Z. Cai, Q. Zhou, Z. Zhang, C. Chen, Bioelectrochemical stimulation of petroleum hydrocarbon degradation in saline soil using U-tube microbial fuel cells, Biotechnol. Bioeng. 109 (2012) 426–433.

[44] B.E. logen, Microbial Fuel Cells, wiley, 2008.

[45] W. Liu, M. Zhang, US EPA3546 method review-microwave accelerated Solvent extraction technique, Modern Scientific Instruments (2005) 52–55.

[46] S. Khashan, S. Dagher, N. Tit, A. Alazzam, I. Obaidat, Novel method for synthesis of Fe 3 O 4 @TiO 2 core/shell nanoparticles, Surf. Coat. Technol. 322 (2017) 92–98.

[47] X. Cui, Y. Zheng, M. Tian, Z. Dong, Novel yolk–shell-structured Fe3O4 @γ-AlOOH nanocomposite modified with Pd nanoparticles as a recyclable catalyst with excellent catalytic activity, Appl. Surf. Sci. 416 (2017) 103–111.

[48] M. Lu, L. Guo, S. Kharkwal, Hn. Wu, H.Y. Ng, S.F.Y. Li, Manganese–polypyrrole–carbon nanotube, a new oxygen reduction catalyst for air-cathode microbial fuel cells, J. Power Sources 221 (2013) 381–386.

[49] B.R. Ringeisen, R. Ray, B. Little, A miniature microbial fuel cell operating with an aerobic anode chamber, J. Power Sources 165 (2007) 591–597.

[50] B. Logan, S. Cheng, V. Watson, G. Estadt, Graphite fiber brush anodes for increased power production in air-cathode microbial fuel cells, Environ. Sci. Technol. 41 (2007) 3341–3346.

[51] A. Paitier, A. Godain, D. Lyon, N. Haddour, T.M. Vogel, J.M. Monier, Microbial fuel cell anodic microbial population dynamics during MFC start-up, Biosens. Bioelectron. 92 (2017) 357–363.

[52] D.H. Park, J.G. Zeikus, Improved fuel cell and electrode designs for producing electricity from microbial degradation, Biotechnol. Bioeng. 81 (2003) 348–355.

[53] J. An, B. Kim, J. Nam, H.Y. Ng, I.S. Chang, Comparison in performance of sediment microbial fuel cells according to depth of embedded anode, Bioresour. Technol. 127 (2013) 138–142.

[54] D.-B. Wang, T.-S. Song, T. Guo, Q. Zeng, J. Xie, Electricity generation from sediment microbial fuel cells with algae-assisted cathodes, Intern. J. Hydrogen Energy 39 (2014) 13224–13230.

[55] Y. Sun, J. Wei, P. Liang, X. Huang, Electricity generation and microbial community changes in microbial fuel cells packed with different anodic materials, Bioresour. Technol. 102 (2011) 10886–10891.

[56] N. Ailijiang, J. Chang, P. Liang, P. Li, Q. Wu, X. Zhang, X. Huang, Electrical stimulation on biodegradation of phenol and responses of microbial communities in conductive carriers supported biofilms of the bioelectrochemical reactor, Bioresour. Technol. 201 (2016) 1–7.

[57] C. Corbella, M. Guivernau, M. Vinas, J. Puigagut, Operational, design and microbial aspects related to power production with microbial fuel cells implemented in constructed wetlands, Water Res. 84 (2015) 232–242.